

LETTER • OPEN ACCESS

Extreme sea level rise along the Indian Ocean coastline: observations and 21st century projections

To cite this article: P Sreeraj *et al* 2022 *Environ. Res. Lett.* **17** 114016

View the [article online](#) for updates and enhancements.

You may also like

- [Attribution of the 2015 record high sea surface temperatures over the central equatorial Pacific and tropical Indian Ocean](#)
In-Hong Park, Seung-Ki Min, Sang-Wook Yeh et al.
- [Multi-decadal modulation of the El Niño–Indian monsoon relationship by Indian Ocean variability](#)
Caroline C Ummenhofer, Alexander Sen Gupta, Yue Li et al.
- [Mechanisms driving ESM-based marine ecosystem predictive skill on the east African coast](#)
Woojin Jeon, Jong-Yeon Park, Charles A Stock et al.



Breath Biopsy® OMNI®

The most advanced, complete solution for
global breath biomarker analysis

TRANSFORM YOUR
RESEARCH WORKFLOW



Expert Study Design
& Management



Robust Breath
Collection



Reliable Sample
Processing & Analysis



In-depth Data
Analysis



Specialist Data
Interpretation

ENVIRONMENTAL RESEARCH
LETTERS

LETTER

OPEN ACCESS

RECEIVED

11 March 2022

REVISED

6 September 2022

ACCEPTED FOR PUBLICATION

6 October 2022

PUBLISHED

24 October 2022

Original content from
this work may be used
under the terms of the
[Creative Commons
Attribution 4.0 licence](#).

Any further distribution
of this work must
maintain attribution to
the author(s) and the title
of the work, journal
citation and DOI.

Extreme sea level rise along the Indian Ocean coastline:
observations and 21st century projectionsP Sreeraj^{1,2} , P Swapna^{1,*} , R Krishnan¹ , A G Nidheesh^{1,3} and N Sandeep^{1,2} ¹ Centre for Climate Change Research, Indian Institute of Tropical Meteorology, Pune, India² Department of Atmospheric and Space Sciences, Savitribai Phule Pune University, Pune, India³ Earth and Life Institute, Université catholique de Louvain, Louvain-la-Neuve, Belgium

* Author to whom any correspondence should be addressed.

E-mail: swapna@tropmet.res.in**Keywords:** extreme sea level, Indian Ocean warming, mean sea-level rise, intensifying tropical cyclonesSupplementary material for this article is available [online](#)

Abstract

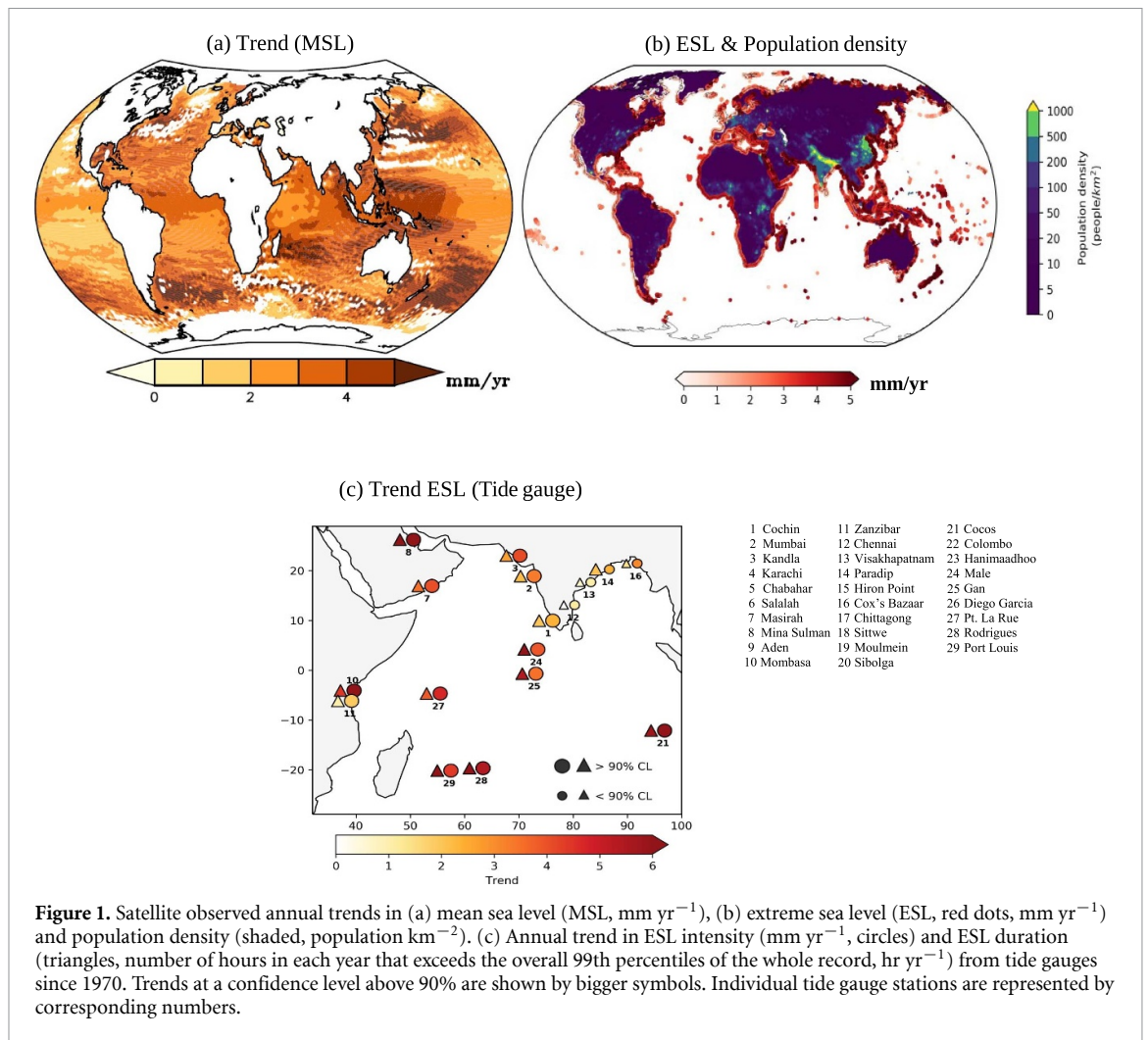
Anthropogenic sea-level rise poses challenges to coastal areas globally. The combined influence of rising mean sea level (MSL) and storm surges exacerbate the extreme sea level (ESL). Increasing ESL poses a major challenge for climate change adaptation of nearly 2.6 billion inhabitants in the Indian Ocean region. Yet, knowledge about past occurrences of ESL and its progression is limited. Combining multiple tide-gauge and satellite-derived sea-level data, we show that ESL has become more frequent, longer-lasting and intense along the Indian Ocean coastlines. We detect a 2–3-fold increase in ESL occurrence, with higher risk along the Arabian Sea coastline and the Indian Ocean Islands. Our results reveal that rising MSL is the primary contributor to ESL increase (more than 75%), with additional contribution from intensifying tropical cyclones. A two-fold increase in ESL along the Indian Ocean coastline is detected with an additional 0.5 °C warming of the Indian Ocean relative to pre-industrial levels. Utilizing the *likely* range (17th–83rd percentile as the spread) of Intergovernmental Panel on Climate Change MSL projections with considerable inter-model spread, we show that the Indian Ocean region will be exposed annually to the present-day 100 year ESL event by 2100, irrespective of the greenhouse-gas emission pathways, and by 2050 under the moderate-emission-mitigation-policy scenario. The study provides a robust regional estimate of ESL and its progression with rising MSL, which is important for climate change adaptation policies.

1. Introduction

Robust assessment of present and projected change in sea level is crucial for climate change adaptation and disaster risk reduction (United Nations Framework Convention on Climate Change 2015). Increasing coastal flood risk from extreme sea level (ESL) is one of the major threats to the global coastline as a consequence of rising mean sea level (MSL). ESL is caused by the combined influence of MSL, astronomical tides and episodic water level fluctuations due to waves and storm surges (Woodworth and Blackman 2004, Pugh and Woodworth 2014). Coastal flooding from ESL can cause severe hazards to densely populated coastal communities and marine ecosystems (Pörtner *et al* 2019, Tebaldi *et al* 2021). Increasing ESL

can pose a major challenge for climate change adaptation to nearly 2.6 billion inhabitants in the Indian Ocean region. Yet, our knowledge about past occurrences of ESL and its progression along the Indian Ocean coastlines and Islands is limited.

Several recent studies that address coastal flooding by ESL at the global scale have shown that ESL changes are driven primarily by the rising MSL (Woodworth and Blackman 2004, Menéndez and Woodworth 2010, Vousdoukas *et al* 2018, Tebaldi *et al* 2021). Oceans absorbed over 90% of the excess heat in the climate system due to anthropogenic warming and have contributed to a rise in the global MSL (Church *et al* 2013, Zanna *et al* 2019). According to the latest Intergovernmental Panel on Climate Change report (IPCC AR6, Fox-Kemper *et al* 2021),



the Indian Ocean sea surface temperature is increasing faster than the global mean. As a result, the MSL rise is accelerating in the Indian Ocean. The spatial trend map of sea-level anomalies (SLAs) from the satellite observation available since 1993 is shown in figure 1(a). The trend map clearly reveals that the MSL rise is higher in the Indian Ocean region. Higher MSL rise is also seen in the western equatorial Pacific and equatorial Atlantic. The MSL rise in the Indian Ocean is 4.6 mm yr⁻¹ and is larger than the global mean (3.5 mm yr⁻¹) based on satellite data since 1993 (figure S1(c)).

The ESL trend along the global coastline from satellite observation (red dots) and population density (shaded, people km⁻²) is shown in figure 1(b). The Indian Ocean coastline is one of the hotspots with an increasing threat to ESL due to very high population density (figure 1(b), shaded), where a higher rise in ESL is seen. In addition, accelerated warming of the Indian Ocean has the potential to increase the intensity of tropical cyclones (TCs) (Knutson *et al* 2010, Murakami *et al* 2017, Balaji *et al* 2018, Vellore *et al* 2020, Deshpande *et al* 2021, Swapna *et al* 2022) which can exacerbate the ESL. Increasing ESL is a threat to the Indian Ocean region as it includes many small

Islands and a vast coastline of approximately 7000 km of India (Ingole 2005). According to the recent IPCC AR6 report (Fox-Kemper *et al* 2021), ESLs that are historically rare will become common, and many low-lying cities and small islands will experience such events annually by 2100. The non-linear interactions between sea-level rise and waves will lead to Islands becoming uninhabitable because of frequent damage to infrastructure and the inability of their freshwater resources (Storlazzi *et al* 2018). Additionally, the identified global 'hotspots' where projected significant change in episodic flooding by the end of the century are mostly concentrated in Asia and northwestern Europe (Kirezci *et al* 2020).

Despite our understanding of global ESL rise, robust regional estimates of ESL and projected change along the densely populated Indian Ocean coastline are lacking. Previous studies on ESL changes along the Indian Ocean coastlines are based on limited tide-gauge (TG) observations (Woodworth and Blackman 2004, Menéndez and Woodworth 2010, Antony *et al* 2016). Early studies based on sea-level observations from the head Bay of Bengal reported the intensification of ESL amplitude (Woodworth and Blackman 2004, Menéndez and Woodworth 2010).

Observational evidence of ESL along the Indian coast is based on three TG stations along the east coast of India for a short duration (Unnikrishnan *et al* 2004, Antony *et al* 2016). Antony *et al* (2016) have shown that ESL variability at selected stations along the east coast of India at inter-annual time scale is dominated by the El Niño Southern Oscillation and the Indian Ocean Dipole. Global model and reanalysis provide regional estimates of ESL (Muis *et al* 2016, 2020, Vousdoukas *et al* 2018). These products reveal that the Indian Ocean ESLs have wide heterogeneity. However, these model estimates have large uncertainty along the Indian Ocean coastline due to insufficient observations.

Here, for the first time, we present a robust regional estimate of ESL along the Indian Ocean coastline using hourly long-term observations from TGs distributed along the Indian Ocean coastlines and Islands, along with high resolution ($0.25^\circ \times 0.25^\circ$) daily satellite data and show that ESLs have already become longer-lasting, more frequent and intense in the Indian Ocean. The study also highlights the projected change in regional ESL over the 21st century along the Indian Ocean coastline, which is crucial for preparing climate change adaptation policies. Our focus is on the regional estimate of ESL and its projected change along the Indian Ocean coastline, including small Island countries. The findings from the study have important implications, given that the Indian Ocean region is inhabited by more than 2 billion people, representing 35% of the world's population.

2. Data and methods

2.1. Data

For this study, we have used hourly sea-level data from 33 TG stations along the Indian Ocean coastline and Indian Ocean Island stations. The Indian TG data is obtained from two agencies, the SOI (1870–2007 period) and the Indian National Centre for Ocean Information Services (INCOIS 2010 to present). Detailed quality control of the TG data has been done. Since the TG data for the Indian coast were obtained from two different sources having different datum, direct merging is not possible. These data were merged by applying break-point alignment techniques using a linear fit in sea-level time series following Boretti (2020). This prevents the inference of incorrect trends in the total records. Quality-controlled sea-level data for the rim countries of the Indian Ocean and Islands were obtained from the University of Hawaii Sea Level Center portal (UHSLC, <https://uhslc.soest.hawaii.edu/>) from 1970 to 2019.

Daily satellite SLA data ($0.25^\circ \times 0.25^\circ$) from CMEMS (<https://marine.copernicus.eu>) since 1993 is also used. This dataset is already corrected by removing the dynamic atmospheric (DAC) or the inverse

barometer effect. Following Lobeto *et al* (2018), DAC is added to the satellite-derived SLA for this study. Glacial isostatic adjustment correction is not included in the satellite and TG data. Monthly sea surface temperature (SST) data from extended reconstructed sea surface temperature (Huang *et al* 2017) for the period 1870–2020 and oceanic heat content (OHC₇₀₀) for upper 700 m depth derived from monthly temperature data from Ishii *et al* (2003) are used to estimate the trends in SST and OHC. The TC data is taken from Cyclone e-Atlas, IMD (www.imdchennai.gov.in/).

2.2. Methods

2.2.1. Percentile analysis and estimation of trends

The ESL intensity is estimated as the 99th percentile of hourly sea level at each year separately following the methodology of Menéndez and Woodworth (2010), Woodworth and Blackman (2004), Feng *et al* (2019), Marcos *et al* (2009). These studies have considered the annual 99th percentiles of hourly sea-level and skew surges as the ESL and extreme skew surge, respectively. Skew surge is the difference between the observed highest water level and the predicted high tide in a tidal cycle, irrespective of the difference in timing between them. Physically it is the flood level above the highest tide in a tidal cycle (Batstone *et al* 2013, Williams *et al* 2016). The duration/count (number) of ESL events for each year is estimated from the number of times ESL values exceeded the 99th percentile threshold of the whole record.

Time series of annual 99th percentile (ESL) and skew surges for each TG are created for trend analysis. For estimating the trends, years with at least 75% of data available were considered, and the trends were estimated based on the Mann-Kendall test (Kendall 1975). To exclude the effect of the 18.6 year nodal cycle of tides (Pugh and Woodworth 2014), only those stations with at least 19 years of data were considered for the trend estimates. The trends in ESL, MSL, skew surges, and the corresponding *P*-values are listed in table S1.

2.2.2. Skew surge computation

The non-tidal residual obtained from hourly sea-level data, after removing the tidal and MSL components, is considered as the storm surge component (Pugh and Woodworth 2014). The non-tidal residual often contains a fraction of leaked tidal signals due to slight phase shift of the predicted tide, which is known as clock error/quasi tidal oscillation. In order to elude the problem of clock error, skew surge is taken as the difference between the observed highest water level and the predicted high tide in a tidal cycle irrespective of the difference in timing between them (Batstone *et al* 2013). Physically, skew surge refers to the flood level above the highest tide in a tidal cycle. Therefore, adding skew surge values with highest tide will give the observed peak sea level in a tidal cycle. To

compute skew surges, hourly sea-level data is separated into tides and non-tidal residuals for each year, using 68 tidal constituents following Foreman (2004). On average, there are 730 tidal cycles; hence 730 skew surge values are obtained in a year. The observed highest water level in a tidal cycle is subtracted from the highest predicted tide in the same cycle, following Mawdsley and Haigh (2016). The highest water level in a tidal cycle may not happen at the highest tidal phase. Thus, a surge which is skewed to the highest tide could cause the highest water level in a tidal cycle, hence called the skew surge. The advantage of skew surge analysis is that it is unaffected by the clock errors in TG data and is more robust than the classical non-tidal residuals.

2.2.3. Extreme value analysis

As a metric of occurrence, event strength is generally expressed in terms of return periods and return levels. Data were linearly detrended to a zero mean relative to the local vertical datum for each station for generating quasi-stationary time series for estimating the return period and return levels of ESL and skew surges. This time-series data is used for generalized extreme value (GEV) analysis following Coles (2001). The GEV distribution is a family of continuous probability distributions developed within the extreme value theory, which provides the statistical framework to make inferences about the probability of very rare or extreme events. Return period and return level of ESL and skew surge are estimated using the r-largest GEV fit to the sea-level data, i.e. r-largest events (1–5) in each year with a three-day gap are fitted to standard GEV distribution. The three-day gap helps to bypass duplicating the same event and hence avoid the overestimation of return levels. The cumulative distribution function of the GEV distribution is given by,

$$f(x, \mu, \sigma, \varepsilon) = e^{\left\{ -\left[1 + \frac{\varepsilon - \mu}{\sigma} \right]^{\frac{-1}{\varepsilon}} \right\}}$$

where the location (μ), scale (σ), and shape (ε) parameters are estimated by the method of moments (Coles 2001) and are shown in table S2. The Kolmogorov–Smirnov (Smirnov 1948) statistical significance test has been done to ensure the fit.

2.2.4. Probability ratio (PR) and fraction of attributable risk (FAR)

The PR can be interpreted as a measure of how the number of ESL days in each year has changed w.r.t. the whole record. Following Frölicher *et al* (2018), the PR is estimated as follows

$$PR = \frac{PR_1}{PR_0}.$$

P_1 is the probability of exceeding a relative threshold (99th percentile) in a year, i.e. the number of days exceeding 99th percentile sea level in a year/total number of days in that year. P_0 is the probability of exceeding that threshold during the entire period, i.e. the number of days that have exceeded the 99th percentile during the whole period/total number of days during the entire period. Thus, PR represents the relative strength of ESL in each year compared to the whole record. It should be noted that the threshold for estimating PR is a constant for P_0 , whereas it can change for P_1 every year. PR, which is greater than 1, implies ESL change in that particular year is more than the local threshold in the whole record and vice versa (the corresponding risk will be more). This risk factor is denoted by the FAR.

The FAR for each year is computed from the PR value as

$$FAR = 1 - \frac{1}{PR}.$$

FAR values vary from 0 to 1 (or 0%–100%) if $PR \geq 1$. If $PR < 1$, which means ESL change is lower than the local threshold, then the risk is considered zero.

3. Results

3.1. Observed increase in ESL along the Indian Ocean coastline

We estimated the long-term trend in the intensity and duration of ESL along the Indian Ocean coastline based on hourly TG observations (figure 1(c)). Since the temporal coverage of TG data is highly varying from one TG to another, we use data from 1970 at selected coastal locations of the Indian Ocean. Statistically significant trends based on Mann-Kendall test are shown by larger symbols. The ESL trend and corresponding P -values are listed in table S1. It can be seen that both ESL intensity (circles, figure 1(c)) and duration (triangles, figure 1(c)) show a significant increase along the Indian Ocean coastline. Statistically significant increasing trends are seen, especially along the west coast of India, western Arabian Sea stations, Southeast African coast and the Island stations of the Indian Ocean. The Island stations include Male, Gan, Diego Garcia, Pt. La Rue, Rodrigues, and Port Louis (Shown in figure 1(c)).

ESL intensity is also estimated along the TG locations using satellite data (figure S2(a)). Satellite-derived SLA are utilized along the TG locations where the correlation between the two datasets is above 0.5, within a circle of radius of 100 km centered to each TG station following the method of Lobeto *et al* (2018). ESL computed from the satellite data excludes tidal information and provides estimates based on MSL and surges. Since sub-daily data is not available from

satellite, the duration of ESL is not estimated. Consistent with TG records, satellite data also show a significant increase in the intensity of ESL along the Indian Ocean coastline. Interestingly, a higher rate of ESL increase is seen along the coastal regions of the Arabian Sea and Island stations of the Indian Ocean (figure S2(a)).

3.2. Spatial distribution of ESL along the Indian Ocean coastline

The trend analysis reveals an increase in ESL along the Indian Ocean coastline. As the ESL trend is non-homogeneous along the Indian Ocean coastline, it is worth analyzing the spatial variability of ESL. We present ESL that could occur 1 in 100 year return period (hereafter, ESL_{100}), above the MSL for each TG location (figure 2(a)). The details of ESL_{100} computation are discussed in section 2. The observed hourly sea-level data for the period 1970–2020 were used for the analysis. It can be noticed that the ESL_{100} along the Indian Ocean coastline possesses larger spatial heterogeneity (with a range of 0.5–4 m above MSL). Lower return levels of ESL_{100} are seen along the southern coast of India and higher values towards the northern Arabian Sea and Bay of Bengal. For example, ESL_{100} in Cochin is 0.8 m, whereas, in Kandla, the value is 3.5 m, following the tidal range, which increases from south to the northern coast of India (The Indian Tide Tables, Geodetic and Research Branch, Survey of India 1964).

In addition, the Island stations in the southern Indian Ocean exhibit higher ESL_{100} as compared to equatorial Indian Ocean stations. Although the ESL_{100} values are smaller at island stations compared to stations along the coastlines of India and other rim countries, the ESL can have significant impacts in the island regions. This is due to the fact that the area that can inundate during an ESL event in the Island region could be larger due to the lower coastal elevation (IPCC AR5). This is further supported by the risk analysis presented in the subsequent section.

The return levels of ESL corresponding to different return periods at selected TG locations on the east and west coasts of India, Indian Ocean rim countries and Island stations are presented in figure 2(b). The red dots are the observed ESL, and the blue line shows the GEV fit. The upper and lower limit (dashed line) represents 95% confidence bounds of ESL. A one in thousand-year return level in Chennai is comparable to a one in a ten-year event at Paradip. Similarly, a thousand-year event in Male in the equatorial Indian Ocean region is comparable to a ten-year event along Cocos Island in the southern Indian Ocean.

3.3. Mechanism contributing to increasing ESL

To understand the mechanism contributing to ESL increase, we analyze the components that contribute to change in ESL. The ESL and its components, MSL,

tide, and skew surge, exhibit strong seasonal variability across different locations; higher ESL is seen during the months of higher MSL and during the peak storminess season (figure S3).

As MSL is considered the major contributor to ESL increase along the global coastline (Menéndez and Woodworth 2010, Tebaldi *et al* 2021), we analyze the long-term changes in MSL along the Indian Ocean coastline. The Indian Ocean is warming faster than the global mean (Fox-Kemper *et al* 2021). The rate of increase in heat content per unit area for the upper 700 m in the Indian Ocean ($0.28 \times 10^8 \text{ Jm}^{-2} \text{ decade}^{-1}$) is higher than the global mean ($0.17 \times 10^8 \text{ Jm}^{-2} \text{ decade}^{-1}$) (figure S1(b)). Accordingly, the MSL rise is also higher in the Indian Ocean compared to the global-MSL rise (figure S1(c)). Previous studies (Unnikrishnan and Shankar 2007, Unnikrishnan *et al* 2015, Swapna *et al* 2017) have shown that MSL is increasing in the north Indian Ocean. The thermal expansion or thermosteric sea-level rise contributes to more than 75% of MSL rise in the north Indian Ocean (Panickal *et al* 2020). The long-term trend in MSL from the TG records shows a significant rise in MSL all along the Indian Ocean coastline (figure 3(a)). The MSL trend and corresponding *P*-values are listed in table S1. Interestingly, a higher rate of MSL rise is seen along the Arabian Sea coastal stations and Island stations, where ESL also shows a significant increasing trend (figure 1(c)).

With the accelerated warming of the Indian Ocean (Alory and Meyers 2009, Roxy *et al* 2020), TC intensity has been increasing in the Indian Ocean, especially in the northern Indian Ocean (Balaji *et al* 2018, Vellore *et al* 2020, Deshpande *et al* 2021, Swapna *et al* 2022). This has led to infrastructure loss and adversely impacted the coastal community. Recently in May 2021, the Indian Ocean witnessed unprecedented consecutive severe TCs, Tauktae in the Arabian Sea and Yaas in the Bay of Bengal (Cyclone e-Atlas, IMD). The Tauktae was an extremely severe cyclonic storm with a maximum wind speed of about 100 knots during landfall, while Yaas was a very severe cyclonic storm with a wind speed of 75 knots during landfall. Both of these systems have rapidly intensified and made landfall along the Indian coast, causing severe damages and fatalities. The tracks of these TC and associated high-water level (HWL) and wind speeds are shown (figure 3(b)). HWL is the maximum sea level recorded in the hourly TG data when the cyclone was closer to the TG locations (Cyclone e-Atlas, IMD). Additionally, observed surge heights at selected TG stations associated with these TC's are also shown in figure 3(b). Both the TC's produced HWL all along the coastline, causing coastal flooding, infrastructure damage and dislocation of a larger proportion of the coastal population. This reveals that ESL events triggered along the Indian Ocean coastline in association with intense TC's can lead

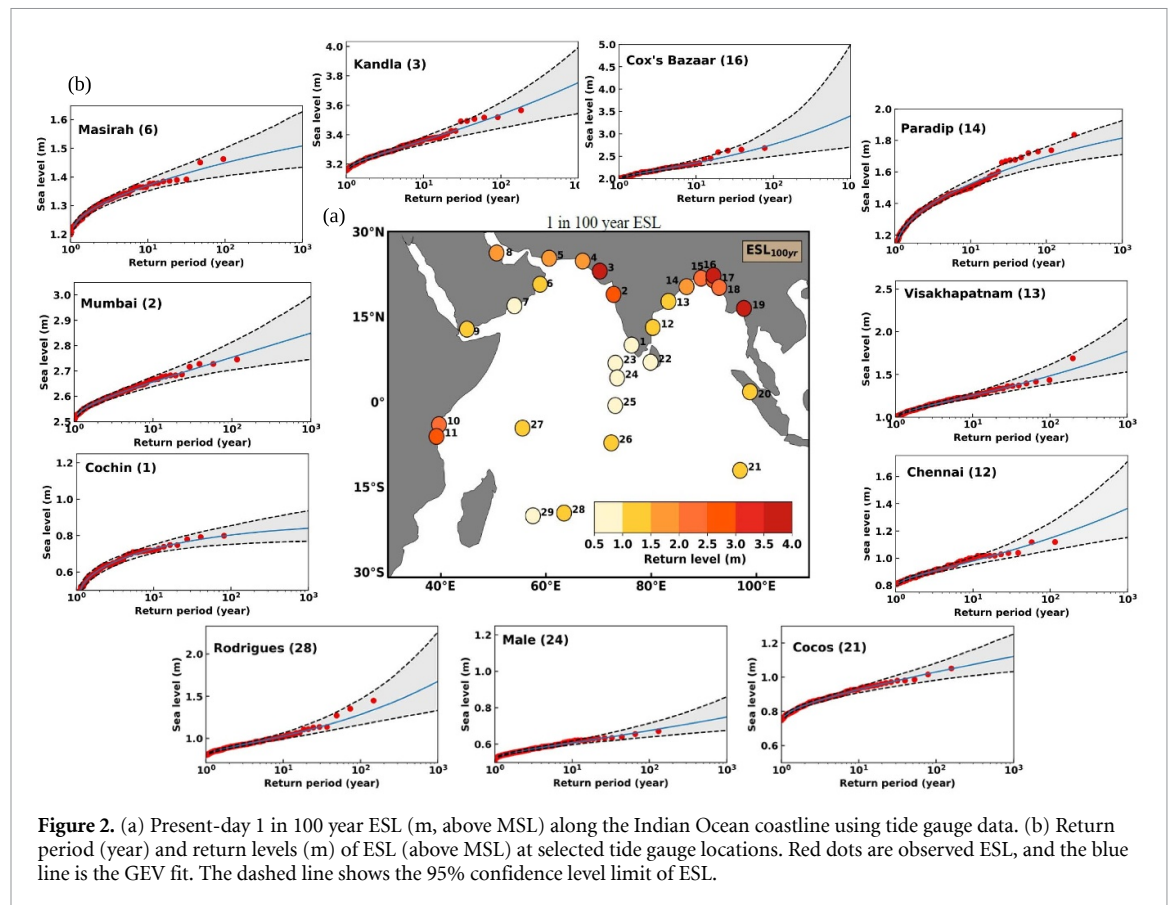


Figure 2. (a) Present-day 1 in 100 year ESL (m, above MSL) along the Indian Ocean coastline using tide gauge data. (b) Return period (year) and return levels (m) of ESL (above MSL) at selected tide gauge locations. Red dots are observed ESL, and the blue line is the GEV fit. The dashed line shows the 95% confidence level limit of ESL.

to coastal flooding and risk along densely populated Indian Ocean coastline.

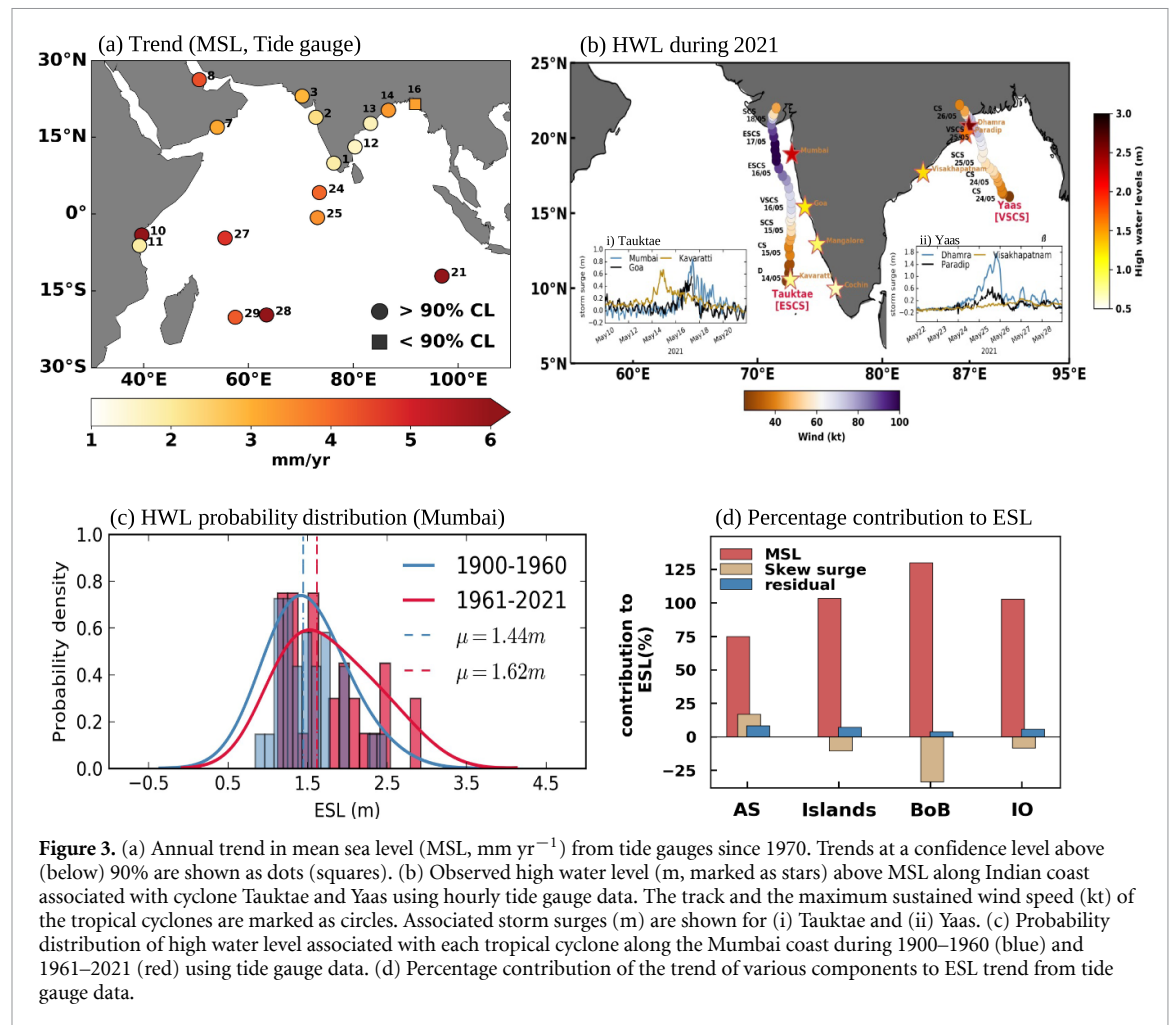
To get insight into long-term changes in ESL associated with an increase in the TC intensity, we estimate the probability of HWL's along the Mumbai coast. Mumbai is a unique station along the Indian Ocean coast where more than 100 years of TG data is available and is also one of the densely populated and economically important metropolitan-city. The probability of HWL's associated with each TC since 1900 is shown (figure 3(c)). The TC data is taken from India Meteorological Department. It can be noted that the probability of higher HWL's (more than 2 m above MSL) has increased in the recent six decades (1961–2020) as compared to 1900–1960. In addition, long-term hourly sea-level data (more than six decades) is also available from other TG locations (Cochin, Chennai, Visakhapatnam, Paradip). We used these data sets to show the long-term trends in the ESL and MSL (figure S2(b)). The results reveal a significant rise in ESL and MSL along these TG stations. The analysis reveals that ESL events are on a rise along the Indian Ocean coastline.

To understand the relative contributors to increasing ESL along the Indian Ocean coastline, we have estimated the trend in intensity of ESL, MSL and skew surges and computed the percentage contributions of MSL to ESL and skew surges to ESL (figure 3(d)). The analysis reveals that the

percentage contribution from the increasing trend in MSL contributes to more than 75% increasing trend in ESL, while skew surges also contribute positively (about 20%) along the Arabian Sea coast. It can be noted that the percentage contribution to the ESL increase in the Bay of Bengal comes mainly from the increase of MSL, whereas the small negative trend of the skew surge intensity component indicate a relatively smaller contributions to ESL changes along the east coast of India and Bay of Bengal (figure 3(d)). The departure from 100% (MSL + skew surge trend) contribution to ESL is considered as the residual in the ESL trend (blue bar shown in figure 3(d)). This could be due to changes in the tide or other non-linear interactions. However, the residual part is found to be small compared to MSL or skew surges. Thus, ESL increase is contributed largely by MSL rise for stations along the Bay of Bengal and Island stations of the Indian Ocean. However, along the coastal stations of the Arabian Sea, both increasing skew surges and MSL contribute to ESL rise. The estimates based on satellite data (figure not shown) also support that MSL rise is the primary contributor to ESL increase in the Indian Ocean.

3.4. Increasing risk associated with ESL

Following Frölicher *et al* (2018), we quantified the annual PR (the fraction by which the number of ESL or frequency changes per year) and FAR (figure 4)

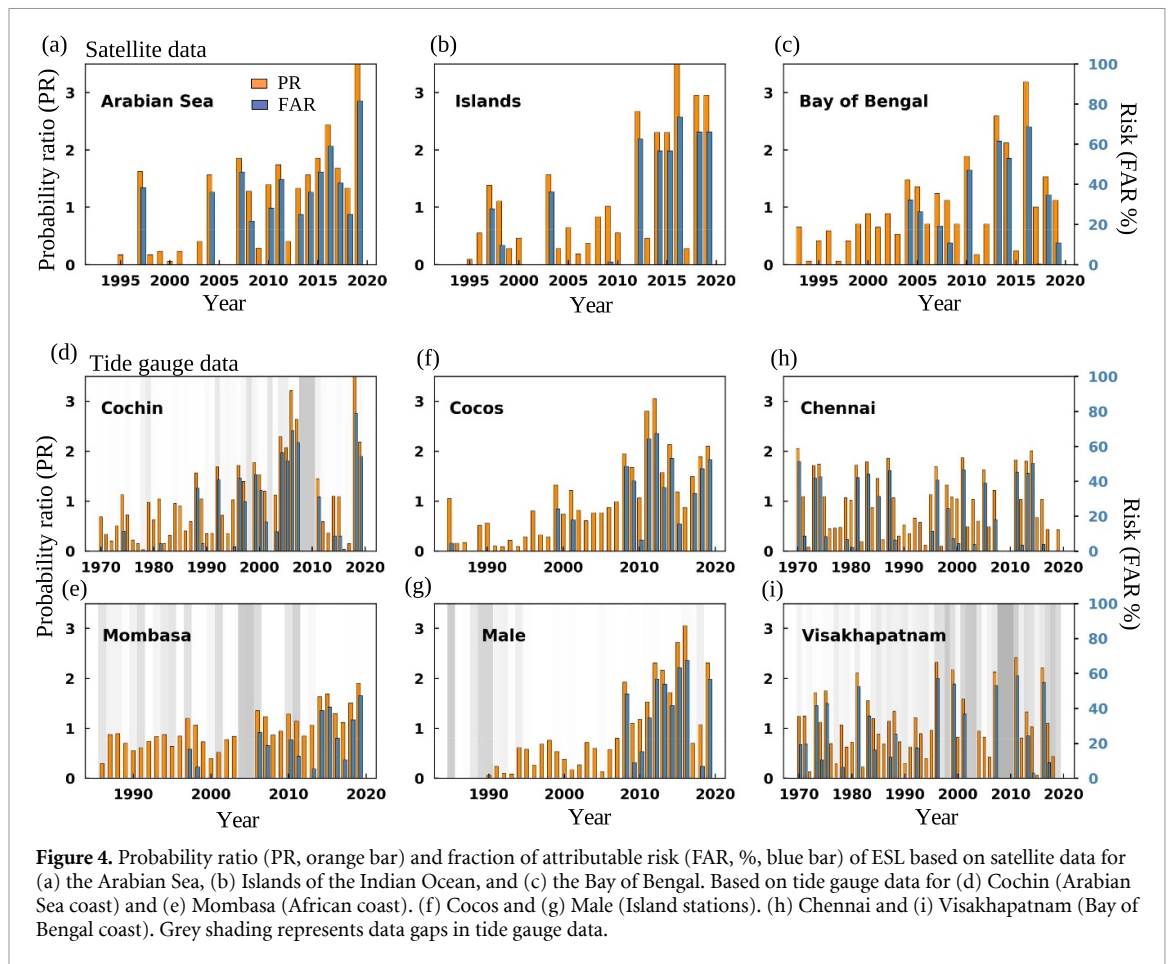


to understand the temporal changes in ESL and associated risk. The PR and FAR are estimated for the coastal stations along the Arabian Sea, Bay of Bengal and Island region of the Indian Ocean from the satellite data (figures 4(a)–(c)) and from TGs (figures 4(d)–(i)). Details about PR and FAR are described in section 2. During the recent three-to-four decades, the probability of occurrence of ESL along the Indian Ocean coastline shows a 2–3-fold increase, especially along the Arabian Sea stations (figures 4(a) and (d)–(e)) and Island stations of the Indian Ocean (figures 4(b) and (f)–(g)). Stations along the Bay of Bengal coastline show an episodic increase in ESL mostly associated with TC events (figures 4(c) and (h)–(i)). The risk associated with ESL (FAR) also shows an increase (more than 50%) in recent decades, especially along the Arabian Sea coast (figure 4(a)).

Along the Island stations of the Indian Ocean, the one in hundred-year ESL values are lower (~ 0.5 m above MSL). However, a 2–3-fold increase in the PR and FAR of ESL has been seen in recent decades (figures 4(b) and (f)–(g)). Alarming, the associated risk, as shown by FAR, has shown a sharp increase by 50%–70% along the Island stations of the Indian

Ocean (figures 4(b) and (f)–(g)). A slight increase in MSL can significantly augment the frequency and intensity of flooding in these regions because of the log-linear relationship between a flood's height and its recurrence interval (Pugh and Woodworth 2014). The potential for compounding effects, like storm surge and high MSL, is of particular concern for the small Islands as they contribute significantly to flood risks, as shown by the sharp increase in FAR along Island stations of the Indian Ocean.

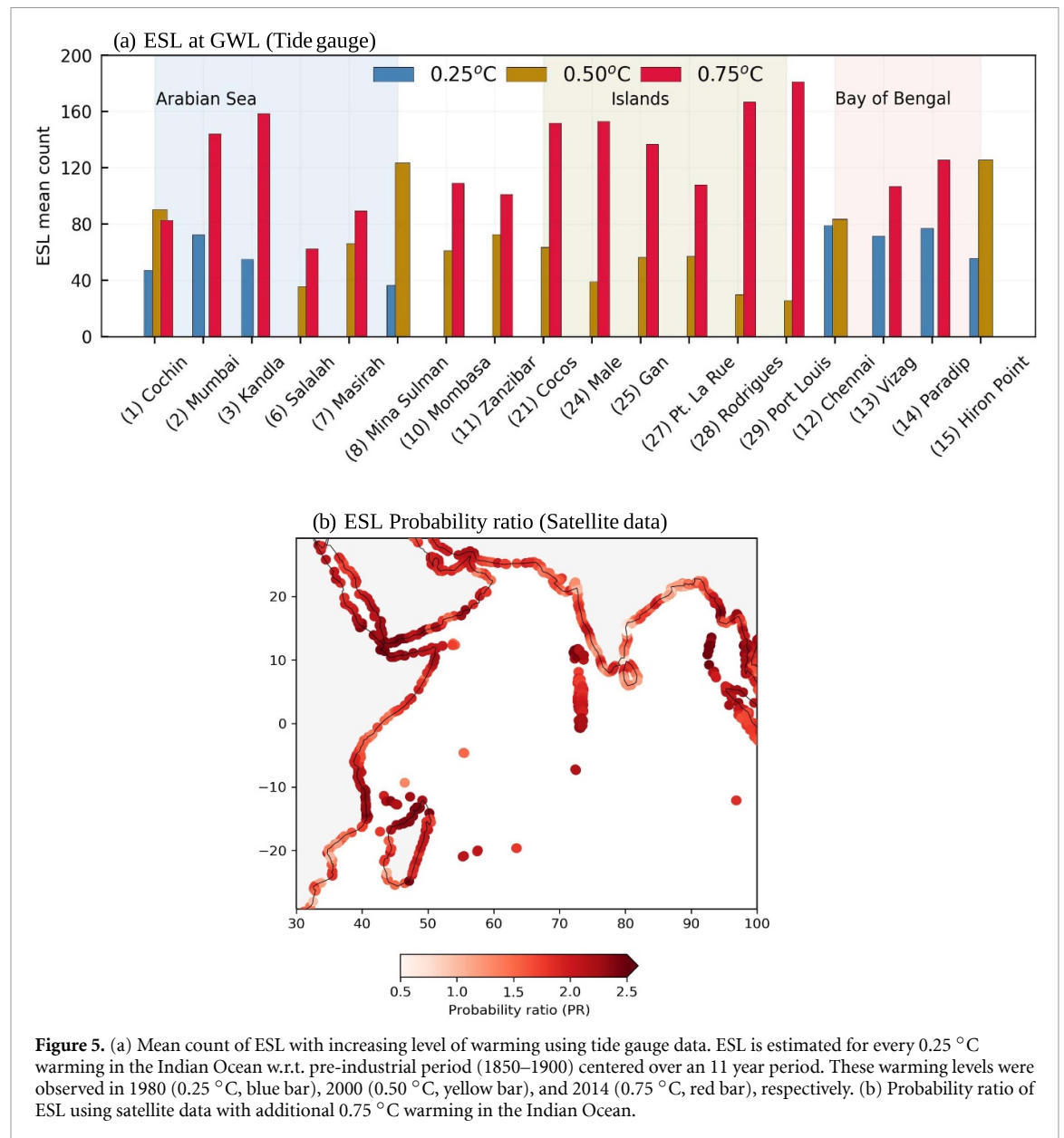
Considering the lower elevation of these Islands and coastal protection facilities, the flooding exposure and inundation need to be mapped in detail. Very Severe Cyclonic Storm Ockhi caused huge damage to the Maldives (Riyas *et al* 2020), and hence future exposure to cyclones cannot be neglected and needs systematic studies. Southern Indian Ocean Islands like Port Louis, Rodrigues (Mauritius), and Cocos (Australia) are faced with historic cyclonic tracks. Thus these regions are all vulnerable to ESL risk in multiple ways. The analysis reveals that the ESL have already become longer-lasting, more frequent, and more intense along the Indian Ocean coastline. Island stations of the Indian Ocean and Arabian Sea coastal regions detect higher risk associated with ESL.



3.5. Increasing frequency of ESL with warming

There is mounting evidence that global warming drives global MSL rise and more frequent ESLs globally. The MSL rise can also be driven by variability arising from different modes of variability like IPO (Zhang *et al* 1997), which is beyond the scope of our present work. A preliminary analysis indicates that IPO influence is seen mostly in the southern and eastern Indian ocean (figure S4(a)). The MSL trend is found to be significant even after removing the IPO-driven MSL trend (figures S4(b) and (c)). A recent study by Tebaldi *et al* (2021) has shown that tropical regions are more prone to ESL at increasing levels of global warming. In order to understand the changes in ESL under warming, we estimate the actual count of ESLs along the Indian Ocean coastline with increasing levels of warming relative to the preindustrial period (1850–1900). We estimate the ESL count (hourly values exceeding the 99th percentile of the whole record) at 0.25 °C, 0.5 °C and 0.75 °C warming levels in the Indian Ocean w.r.t. the pre-industrial period. The warming levels were estimated by averaging the 11 year running mean of Indian Ocean SST (40°E–100°E and 30°S–30°N) and calculating the difference w.r.t. pre-industrial period (figure S1(d)). The mean count of ESL occurrence over an 11 year period centered around the warming levels 0.25 °C (blue), 0.5 °C (yellow) and 0.75 °C

(red), which corresponds to 1975–1985, 1995–2005, 2009–2019, respectively, are estimated and is shown in figure 5(a). Thus, the ESL count under 0.75 °C warming is the mean count from 2009 to 2019 and, respectively, for the other cases. A 75% data availability criterion has been chosen to ensure the quality of ESL counts. At certain times, TGs at various locations may not satisfy the data availability threshold criteria and such data points are not considered in our analysis. We notice a 2–3-fold increase in ESL along the Island stations of the Indian Ocean, with additional warming of 0.25 °C, observed between 1995 and 2019 (figure 5(a)). With a 0.25 °C increase in warming level, stations along the west coast of India show a two-fold increase, consistent with our previous analysis (figure 4). Other stations along the Arabian Sea coast also show an increase in ESL with increasing warming (figure 5(a)). The TG estimates are supported by the satellite data (figure 5(b)) showing the mean PR of ESL at 0.75 °C (centered at 2014) warming in the Indian Ocean w.r.t. preindustrial period. Here P_1 is the count of days during 2009–2019 (11 years) that exceeded the 99th percentile of the whole record/total number of days during the 11 year period. P_0 is the ratio of the total number of ESL days exceeding the 99th percentile of the whole record and the total number of days in the whole record (since 1993). Higher PR of ESL events and



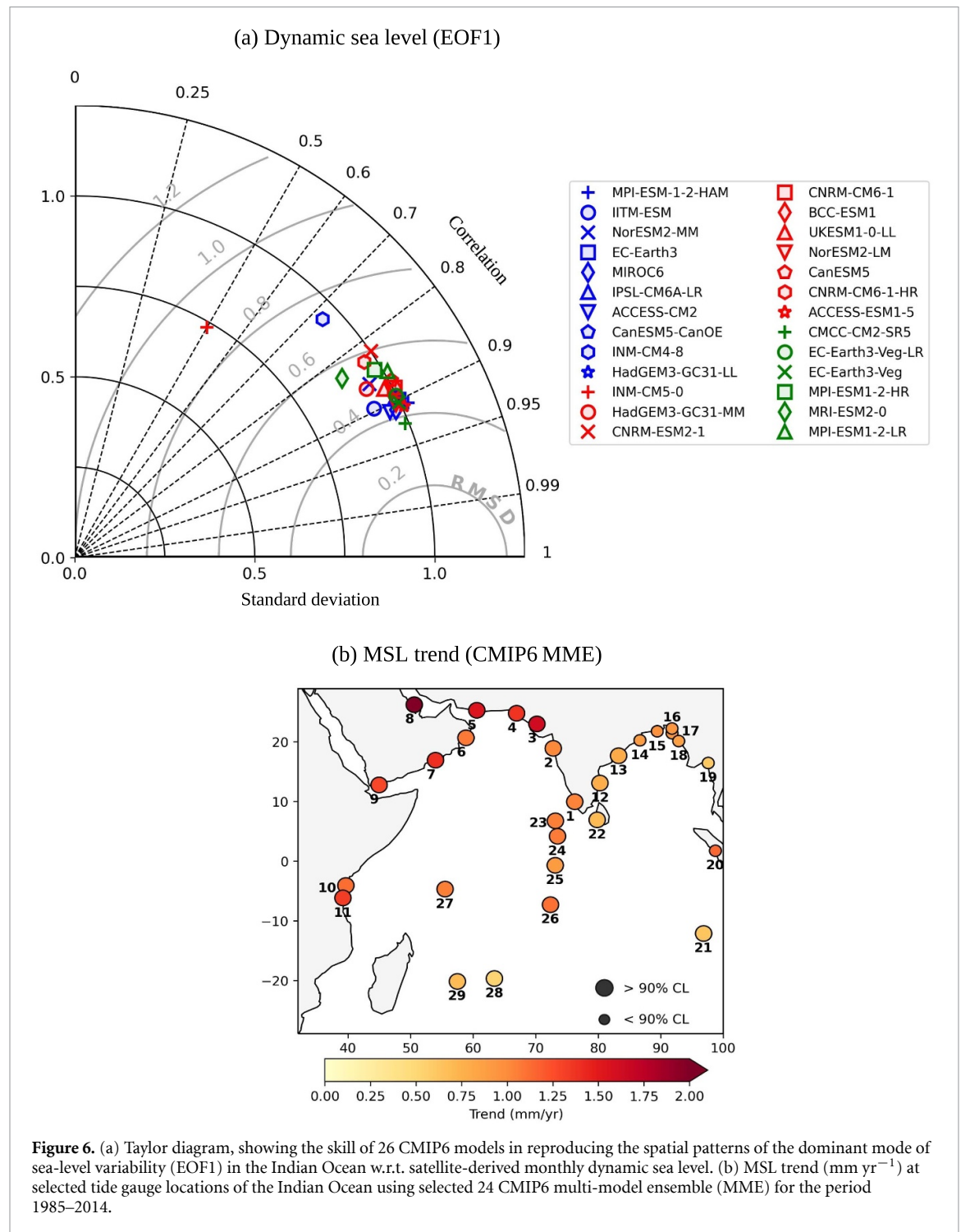
higher risk is seen in the Indian Ocean with increasing levels of warming, especially along the Island stations and coastal regions of the Arabian Sea, with present-day warming of 0.75 °C relative to the pre-industrial period (figure 5(b)).

3.6. Projected changes in ESL along the Indian Ocean coastline

The ESL events have already become intense, frequent and longer-lasting along the Indian Ocean coastline. The percentage contribution of MSL to ESL trend based on both TG data and satellite data shows that MSL trend contributes to more than 75% of the increasing trend in ESL (figure 3(d)). The focus here is to address how the ESL events will amplify with rising MSL along the Indian Ocean coastline. Since we cannot estimate ESL based on available monthly sea-level data from Coupled Model Intercomparison Project Phase 6 (CMIP6) models, we have added observed

estimates of the 100 year ESL event (the extreme total water level expected to be experienced on average once in 100 years based on TG data) to MSL projections from CMIP6 MME, at the TG locations along the Indian Ocean coastline to calculate future ESL_{100} . Values of MSL were obtained from the IPCC AR6 projections taken from IPCC AR6 Sea Level Projection Tool (https://sealevel.nasa.gov/data_tools/17).

Before using the IPCC AR6 projections of CMIP6 models for estimating the future changes in ESL, we analyzed the historical sea-level simulations from CMIP6 models to assess their fidelity in simulating the present-day sea-level variability and trend in the Indian Ocean. Satellite-derived monthly dynamic sea level (DSL) is used as the observation. The sea-level data from 26 CMIP6 models (table S3) used for the assessment of sea-level projections in the IPCC AR6 have been utilized. Only the first realization from each model is used to give equal weightage to all the



models. All the model data are re-gridded onto a uniform $1^\circ \times 1^\circ$ grid for ease of comparison and to compute the multi-model mean (MME) of these models.

The DSL derived from the model sea surface height above the geoid (zos) by removing its time-dependent global mean is utilized to assess the sea-level variability. The CMIP6 DSL is evaluated using mean ocean dynamic topography derived from satellite data (www.aviso.altimetry.fr/en/home.html). The historical simulations of CMIP6 models are used for the last 30 year period (1985–2014) and the altimeter data for the period 1993–2020. The dominant

mode of sea-level variability in the Indian Ocean is obtained based on the empirical orthogonal functions (EOF) analysis of monthly SLAs in the Indian Ocean for each model and observation. The pattern correlation between CMIP6 models and observation of the dominant mode of sea-level variability is shown in figure 6. The patterns of the dominant mode of sea-level variability in the Indian Ocean are captured reasonably well by the CMIP6 models (figure 6(a)). The EOF pattern from individual models is shown in figure S5. Details of the model used and its skill scores are listed in table S3. Except for two models

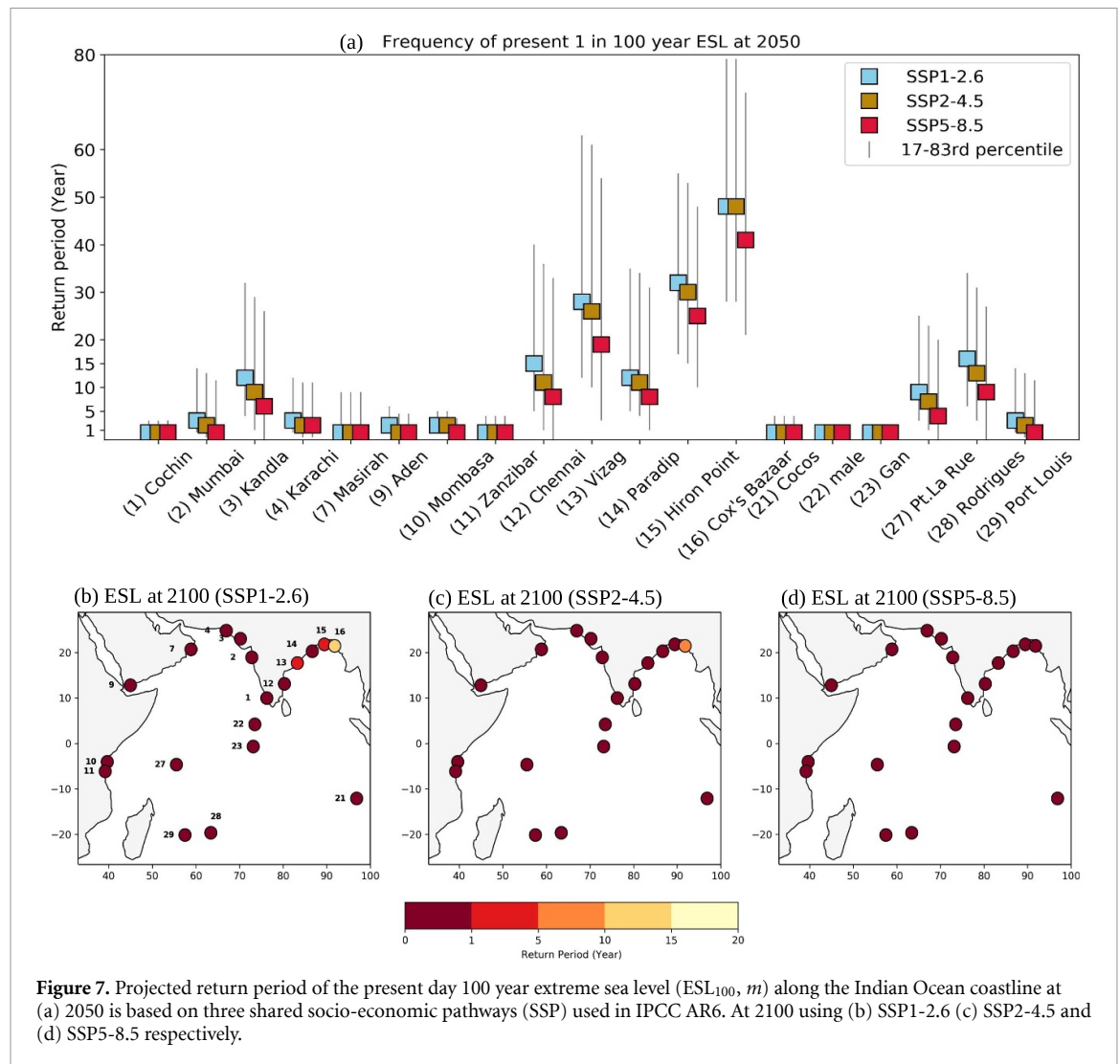


Figure 7. Projected return period of the present day 100 year extreme sea level (ESL_{100}, m) along the Indian Ocean coastline at (a) 2050 is based on three shared socio-economic pathways (SSP) used in IPCC AR6. At 2100 using (b) SSP1-2.6 (c) SSP2-4.5 and (d) SSP5-8.5 respectively.

(INM-CM4-8 and INM-CM5-0), most of the CMIP6 models exhibit more than 0.8 correlation with observation and normalized standard deviation between 0.9 and 1.1 in the Indian Ocean region. All these models (except INM-CM4-8 and INM-CM5-0) with skill scores of more than 0.96 are used for assessing the sea-level trend in the Indian Ocean.

For assessing the long-term trend in MSL, we have used de-drifted CMIP6 sea-level data. The model drift at each grid point is estimated by fitting a quadratic polynomial to the full time series of the preindustrial simulation (Gupta *et al* 2013), and the historical simulation is then de-drifted by subtracting the estimated drift from the preindustrial simulation. We have utilized the de-drifted data from IPCC archive (Fox-Kemper *et al* 2021). The global ocean thermal expansion (zostoga) is added to zos and is used for estimating the sea-level trend along the TG locations. The MSL is averaged within a $1^\circ \times 1^\circ$ grid centered on each TG station, and the trend is estimated based on the multi-model mean (MME) SLAs from the selected CMIP6 models for the period 1985–2014 and is shown in figure 6(b). It can be

noticed that the spatial pattern of the MSL trend from CMIP6 MME is similar to the observed pattern, though trend values are lower compared to observed estimates (figures 3(a) and S2 (b)). Higher MSL rise is seen along the west coast of India and Arabian Sea coastal stations than over the eastern coast of India, similar to the observations. A recent study by Chatterjee and Sajidh (2022) has shown the fidelity of CMIP6 models in capturing the mean state and variability of CMIP models in the Indian Ocean as compared to satellite observations.

The analysis shows that CMIP6 models show fidelity in capturing the observed variability and trend in sea level in the Indian Ocean. These models are utilized for estimating future changes in ESL. The MSL values for the three IPCC Shared Socioeconomic Pathways (SSPs), SSP1-2.6, SSP2-4.5 and SSP5-8.5, are used. The MSL values under these scenarios for 2100 and 2050 along Indian Ocean TG locations are presented in table S4. These SSP scenarios are chosen as SSP1-2.6 represents the low end of the range of plausible future pathways and depicts the 'best case' future from the sustainability

perspective, SSP2-4.5 is the medium part of the range of plausible future pathways representing moderate-emission-mitigation-policy scenario, and SSP5-8.5 represents the high end of plausible future pathways with emissions high enough to produce the 8.5 W m^{-2} radiative forcing by 2100 (O'Neill *et al* 2016). We have used the 17th–83rd percentile as the spread in sea-level projections representing the *likely range* following the methodology used by IPCC AR6 Fox-Kemper *et al* (2021). The 17th–83rd percentile results are interpreted as *likely* ranges, which refer to a probability of at least 66% (i.e. one standard deviation from the mean value).

The projected ESL_{100} along the Indian Ocean coastline is shown in figure 7, utilizing the IPCC *likely range* projections of MSL. The ESL expected to be experienced one in 100 year (ESL_{100}) historically will occur annually or less than a year by 2100 along the Indian Ocean coastline, under all the three scenarios considered, including the low-emission strong mitigation scenario (SSP1-2.6) as seen from figures 7(b)–(d). It has to be noted that the MSL projections from CMIP6 models exhibit considerable inter-model spread, as seen in figure 7(a). The results also reveal that the present ESL_{100} event will occur annually along the Indian Ocean coastline by 2050 (figure 7(a)), even under SSP2-4.5, especially along the Arabian Sea coastline and the Indian Ocean Islands; however, with a large inter-model spread. Previous estimates of ESL based on model studies have identified the Asian region as one of the hot-spots of increasing ESL. We show that ESL_{100} can occur annually along the Indian Ocean coastline by 2050 even under a moderate-emission-mitigation-policy scenario (SSP2-4.5) and by 2100 under all the possible future trajectories of greenhouse gas emission (GHG) including the low-emission strong mitigation scenario (SSP1-2.6). The study highlights an important policy-relevant message: strong mitigation and adaptation measures are needed along the Indian Ocean coastline as ESL_{100} events can occur annually or even less than a year along the densely populated coastline, irrespective of the future GHG emission pathways and socio-economic conditions.

4. Summary and caveats

Increasing coastal flood risk from ESLs is one of the major threats to the global coastline. ESL events have been identified along the global coastline. However, the ESL trend map (figure 1(b)) shows that the Indian Ocean region is one of the hotspots with the rise in ESL, where population density is higher as compared to other global regions. Despite our understanding of the global MSL rise (Church *et al* 2013, Frederikse *et al* 2020) and the contributing processes, regional estimates of ESL and its long-term changes are limited. We present robust regional estimates of

ESL based on multiple TG records distributed all along the Indian Ocean coastline and Islands and also utilizing satellite-derived sea-level observations. The study provides valuable insight into the regional changes in ESL and its projections along the densely populated Indian Ocean coastline, which is vital for preparing adaptation measures.

Accelerated warming of the Indian Ocean (Alory and Meyers 2009, Roxy *et al* 2020) and MSL rise (Unnikrishnan and Shankar 2007, Unnikrishnan *et al* 2015, Swapna *et al* 2017) along with the increasing intensity of TC (Knutson *et al* 2010, Murakami *et al* 2017, Balaji *et al* 2018, Vellore *et al* 2020, Deshpande *et al* 2021, Swapna *et al* 2022) can exacerbate coastal flooding by generating ESL. However, understanding of the long-term changes in ESL and their progression in the Indian Ocean is lacking. Using hourly sea-level observations available from multiple TG along the Indian Ocean coastlines and Island stations and daily satellite-derived sea-level data, we show that the ESLs have already become more frequent, longer lasting and intense in the Indian Ocean. We detect a 2–3-fold increase in ESL and higher risk along the Indian Ocean coastline, especially along the Arabian Sea coastal regions and Island stations. The MSL rise is the primary contributor to ESL increase along the Indian Ocean coastline. The increasing intensity of TC also contributes along the Arabian Sea coast.

Our study highlights that by the end of the century, all of the Indian Ocean coastlines, including Island stations, will experience the present-day 100 year ESL event at least once a year, even for a low emission greenhouse gas trajectory (figures 7(b)–(d)). It has to be noted that the MSL projections from CMIP6 models exhibit considerable inter-model spread, as seen in figure 7(a). We find that most of the locations along the Arabian Sea coast and equatorial Islands in the Indian Ocean will experience present-day 100 year ESL annually by 2050, even under the moderate-emission-mitigation-policy scenario (figure 7(a)). Results from the study caution against the projected increase in ESL and show that the Indian Ocean coastal regions are under increasing risk of coastal flooding by the increasing intensity and frequency of ESL.

The limitation of the study arises from the limited long-term (more than 50 years) observations with higher spatial coverage along the Indian Ocean coastline. This limits our study in understanding century-scale changes in ESL. The ESL in our study considered the still water level only (i.e. a combination of MSL, tide and surge). The effect of waves is not included in the study. The MSL projections in the study are based on the CMIP6 models with considerable intermodal spread. Despite these caveats, our study provides robust regional estimates of historical ESL and its projections along the Indian Ocean coastline, where long-term ESL and MSL estimates

are lacking. Our study highlights increasing ESL along the Indian Ocean coastline and has important policy and practical implications. Increasing ESL along the Indian Ocean coastline urge for raising flood defences along densely populated coastal regions of developing countries and Islands of the Indian Ocean.



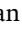

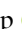
Data availability statement

The data that support the findings of this study are kept in <https://zenodo.org/record/6600183#.Ypbs5jlBxl8>.

Acknowledgments

The authors thank Director IITM for providing support to carry out this research. The authors also thank Indian National Centre for Ocean Information Services (INCOIS) and Survey of India for providing high-frequency sea-level data along the Indian coast and UHSLC for data along Indian Ocean Rim countries. The first author is funded with a research fellowship by the CSIR, Gov. India. We acknowledge the sea-level rise projections tool, NASA and WCRP CMIP6 for the sea-level projections and also Fox-Kemper et al (2021) for the de-drifted sea-level data from CMIP6 models. We thank Dr S R Shetye for the discussions.

ORCID iDs

P Sreeraj  <https://orcid.org/0000-0002-4233-6202>
 P Swapna  <https://orcid.org/0000-0002-7441-7496>
 R Krishnan  <https://orcid.org/0000-0003-0433-7818>
 A G Nidheesh  <https://orcid.org/0000-0002-3598-1107>
 N Sandeep  <https://orcid.org/0000-0001-9528-5675>

References

- Alory G and Meyers G 2009 Warming of the upper equatorial Indian Ocean and changes in the heat budget (1960–99) *J. Clim.* **22** 93–113
- Antony C, Unnikrishnan A S and Woodworth P L 2016 Evolution of extreme high waters along the east coast of India and at the head of the Bay of Bengal *Glob. Planet. Change* **140** 59–67
- Balaji M, Chakraborty A and Mandal M 2018 Changes in tropical cyclone activity in north Indian Ocean during satellite era (1981–2014) *Int. J. Climatol.* **38** 2819–37
- Batstone C, Lawless M, Tawn J, Horsburgh K, Blackman D, McMillan A, Worth D, Laeger S and Hunt T 2013 A UK best-practice approach for extreme sea-level analysis along complex topographic coastlines *Ocean Eng.* **71** 28–39
- Boretti A 2020 Analysis of segmented sea level time series *Appl. Sci.* **10** 625
- Chatterjee A and Sajidh C K 2022 Indian Ocean dynamic sea level, variability and projections *CMIP6 Models* (<https://doi.org/10.21203/rs.3.rs-1192038/v1>)
- Church J A et al 2013 Sea level change *Climate Change 2013: The Physical Science Basis. Contribution of Working Group I to the Fifth Assessment Report of the Intergovernmental Panel on Climate Change* ed T F Stocker et al (Cambridge: Cambridge University Press) pp 1137–1
- Coles S 2001 *An Introduction to Statistical Modeling of Extreme Values* vol 208 (Berlin: Springer)
- Deshpande M, Singh V K, Ganadhi M K, Roxy M K, Emmanuel R and Kumar U 2021 Changing status of tropical cyclones over the north Indian Ocean *Clim. Dyn.* **57** 3545–67
- Feng J, Li D, Wang T, Liu Q, Deng L and Zhao L 2019 Acceleration of the extreme sea level rise along the Chinese coast *Earth Space Sci.* **6** 1942–56
- Foreman M 2004 *Manual for Tidal Currents Analysis and Prediction* vol 78
- Fox-Kemper B et al 2021 Ocean, cryosphere and sea level change *Climate Change 2021: The Physical Science Basis. Contribution of Working Group I to the Sixth Assessment Report of the Intergovernmental Panel on Climate Change* (Cambridge University Press)
- Frederikse T et al 2020 The causes of sea-level rise since 1900 *Nature* **584** 393–7
- Frölicher T L, Fischer E M and Gruber N 2018 Marine heatwaves under global warming *Nature* **560** 360–4
- Gupta A S, Jourdain N C, Brown J N and Monselesan D 2013 Climate drift in the CMIP5 models *J. Clim.* **26** 8597–615
- Huang B, Thorne P W, Banzon V F, Boyer T, Chepurin G, Lawrimore J H, Menne M J, Smith T M, Vose R S and Zhang H-M 2017 Extended reconstructed sea surface temperature, version 5 (ERSSTv5): upgrades, validations, and intercomparisons *J. Clim.* **30** 8179–205
- Ingole B 2005 Indian Ocean coasts, coastal ecology *Encyclopedia of Coastal Science* ed M L Schwartz (Dordrecht: Springer) pp 546–54
- Ishii M, Kimoto M and Kachi M 2003 Historical Ocean subsurface temperature analysis with error estimates *Mon. Weather Rev.* **131** 51–73
- Kendall M G 1975 *Rank Correlation Methods* 4th edn (London: Charles Griffin)
- Kirezci E, Young I R, Ranasinghe R, Muis S, Nicholls R J, Lincke D and Hinkel J 2020 Projections of global-scale extreme sea levels and resulting episodic coastal flooding over the 21st century *Sci. Rep.* **10** 11629
- Knutson T R, McBride J L, Chan J, Emanuel K, Holland G, Landsea C, Held I, Kossin J P, Srivastava A K and Sugi M 2010 Tropical cyclones and climate change *Nat. Geosci.* **3** 157–63
- Lobato H, Menendez M and Losada I J 2018 Toward a methodology for estimating coastal extreme sea levels from satellite altimetry *J. Geophys. Res.* **123** 8284–98
- Marcos M, Tsimplis M N and Shaw A G P 2009 Sea level extremes in southern Europe *J. Geophys. Res.* **114**
- Mawdsley R J and Haigh I D 2016 Spatial and temporal variability and long-term trends in skew surges globally *Front. Mar. Sci.* **3** 29
- Menéndez M and Woodworth P L 2010 Changes in extreme high water levels based on a quasi-global tide-gauge data set *J. Geophys. Res.* **115**
- Muis S, Irazoqui M, Dullaart J, Rego J, Madsen K, Su J, Yan K and Verlaan M 2020 A high-resolution global dataset of extreme sea levels, tides, and storm surges, including future projections *Front. Mar. Sci.* **7** 263
- Muis S, Verlaan M, Winsemius H C, Aerts J C J H and Ward P J 2016 A global reanalysis of storm surges and extreme sea levels *Nat. Commun.* **7** 11969
- Murakami H, Vecchi G A and Underwood S 2017 Increasing frequency of extremely severe cyclonic storms over the Arabian Sea *Nat. Clim. Change* **7** 885–9
- O'Neill B C et al 2016 The scenario model intercomparison project (ScenarioMIP) for CMIP6 *Geosci. Model Dev.* **9** 3461–82
- Panickal S et al 2020 Sea-level rise pp 175–89
- Pörtner H-O et al N M W (eds) 2019 *IPCC Special Report on the Ocean and Cryosphere in a Changing Climate* (Press)

- Pugh D and Woodworth P 2014 *Sea-level Science: Understanding Tides, Surges Tsunamis and Mean Sea-level Changes* (Cambridge: Cambridge University Press) p 407
- Riyas C, Idreesbabu K K, Marimuthu N and Sureshkumar S 2020 Impact of the tropical cyclone Ockhi on ecological and geomorphological structures of the small low-lying Islands in the central Indian Ocean Reg. Stud. Mar. Sci. **33** 100963
- Roxy M K et al 2020 Indian Ocean warming *Assessment of Climate Change over the Indian Region: A Report of the Ministry of Earth Sciences (MoES), Government of India* ed R Krishnan et al (Singapore: Springer) pp 191–206
- Smirnov N 1948 Table for estimating the goodness of fit of empirical distributions *Ann. Math. Stat.* **19** 279–81
- Storlazzi C D et al 2018 Most atolls will be uninhabitable by the mid-21st century because of sea-level rise exacerbating wave-driven flooding *Sci. Adv.* **4** eaap9741
- Swapna P, Jyoti J, Krishnan R, Sandeep N and Griffies S M 2017 Multidecadal weakening of Indian summer monsoon circulation induces an increasing Northern Indian Ocean sea level *Geophys. Res. Lett.* **44** 10560–72
- Swapna P, Sreeraj P, Sandeep N, Jyoti J, Krishnan R, Prajeesh A G, Ayantika D C and Manmeet S 2022 Increasing frequency of extremely severe cyclonic storms in the North Indian Ocean by anthropogenic warming and Southwest monsoon weakening *Geophys. Res. Lett.* **49** e2021GL094650
- Tebaldi C, Ranasinghe R, Vousdoukas M, Rasmussen D J, Vega-Westhoff B, Kirezci E, Kopp R E, Sriver R and Mentaschi L 2021 Extreme sea levels at different global warming levels *Nat. Clim. Change* **11** 746–51
- The Indian Tide Tables. Geodetic and Research Branch, Survey of India 1964
- Unnikrishnan A S, Nidheesh A G and Lengaigne M 2015 Sea-level-rise trends off the Indian coasts during the last two decades *Curr. Sci.* **108** 966–70
- Unnikrishnan A S and Shankar D 2007 Are sea-level-rise trends along the coasts of the north Indian Ocean consistent with global estimates? *Glob. Planet. Change* **57** 301–7
- Unnikrishnan A S, Sundar D and Blackman D 2004 Analysis of extreme sea level along the east coast of India *J. Geophys. Res.* **109** 1–7
- Vellore R K, Deshpande N, Priya P, Singh B B, Bisht J, Ghosh S 2020 Extreme storms *Assessment of Climate Change over the Indian Region: A Report of the Ministry of Earth Sciences (MoES), Government of India* ed R Krishnan et al (Singapore: Springer) pp 155–73
- Vousdoukas M I, Mentaschi L, Voukouvalas E, Verlaan M, Jevrejeva S, Jackson L P and Feyen L 2018 Global probabilistic projections of extreme sea levels show intensification of coastal flood hazard *Nat. Commun.* **9** 1–12
- Williams J, Horsburgh K J, Williams J A and Proctor R N F 2016 Tide and skew surge independence: new insights for flood risk *Geophys. Res. Lett.* **43** 6410–7
- Woodworth P L and Blackman D L 2004 Evidence for systematic changes in extreme high waters since the mid-1970s *J. Clim.* **17** 1190–7
- Zanna L, Khatiwala S, Gregory J M, Ison J and Heimbach P 2019 Global reconstruction of historical ocean heat storage and transport *Proc. Natl Acad. Sci.* **116** 1126–31
- Zhang Y, Wallace J M and Battisti D S 1997 ENSO-like interdecadal variability: 1900–93 *J. Clim.* **10** 1004–20